

Supporting Information

Reversible Room Temperature Phosphorescence/ Delayed Fluorescence Switch Triggered by Solvent Exchange in a Ca-based Coordination Polymer

*Ai-Yun Ni, He Zhao, Pei-Pei Zhang, Bo-Lun Zhang, Jian-Jun Zhang, * Shuqin Liu, Jun Ni and Chunying*

*Duan**

Experimental Section

Materials and instrumentation

All reagents were purchased of analytical grade and used as received without further purification. Infrared spectra (IR) were recorded on Nicolet-20DXB spectrometer as KBr pellets in the range of 4000–400 cm⁻¹. ESI mass spectra were recorded using LCQ-Tof MS mass spectrometer (Samples were deprotonated using NaAc). NMR spectra were recorded at ambient temperature on a Bruker Avance II 400M spectrometer. Thermogravimetric analysis (TGA) were performed under nitrogen atmosphere with a heating rate of 10 °C/min using a TA-Q50 thermogravimetric analyzer. Elemental analyses (C, H, N) were determined on Vario EL III Elemental Analyzer. X-ray powder diffraction (XRD) patterns were collected with a D/MAX-2400 diffractometer using Cu- K_{α} radiation ($\lambda = 1.54056 \text{ \AA}$) under ambient conditions. Luminescence spectra were acquired at ambient temperature with solid-state samples by using a HITACHI F-7000 fluorescence spectrophotometer.

Synthesis of 5-(5,7-dioxopyrrolo[3,4-f]benzimidazole-6-yl)isophthalic acid (H₃L)

A mixture of benzimidazole-5,6-dicarboxylic acid (4.12 g, 20 mmol) and 5-aminoisophthalic acid (3.62 g, 20 mmol) in 120 ml DMF was heated at 140 °C for 8 h, then filtrated. The product was washed firstly with DMF, then with EtOH and dried in air. Yield: 66 %. The ligand was used for the synthesis of MOFs without further purification. IR (KBr pellet, cm⁻¹): 3382(m), 3231(w), 3104(w), 2926(w), 2498(w), 1768(s), 1714(vs), 1654(s), 1618(w), 1378(vs), 1256(vs), 1110(s), 837(m), 757(s), 681(m), 614(m). Negative ESI-MS (m/z): 350.0 (H₃L-H⁺), 372.1(H₃L -2H⁺+Na⁺), 174.5((H₃L-2H⁺)/2). Element analysis (%) calcd for C₁₇H₉N₃O₆: C 58.13, H 2.58, N 11.96; found: C 58.34, H 2.35, N 11.90. ¹H-NMR (DMSO-*d*₆, 500 MHz, δ[ppm]): 13.41 (s, 2H), 8.59 (s, 1H), 8.49 (t, *J* = 1.5 Hz, 1H), 8.27 (s, 2H), 8.15 (s, 2H), Melting points: above 300 °C.

Synthesis of [Ca(HL)(DMSO)₂]·DMSO (1)

H₃L (7.0 mg, 0.02 mmol) and CaCl₂ (8.9 mg, 0.08 mmol) were dissolved in a solvent mixture of DMSO/DMF/H₂O(4:4:1, 3.5 mL) in a 20 ml scintillation vial, which was heated to 85 °C for 24 h, then 105 °C for 48 h and cooled to room temperature. The colorless block crystals were collected by filtration, washed with DMSO and dried in air (40% yield based on H₃L). Element analysis (%) calcd for C₂₃H₂₅CaN₃O₉S₃: C 44.29, H 4.04, N 6.74; found: C 44.04, H 4.09, N 6.44. IR (KBr pellet, cm⁻¹): 3423(br), 3180(br), 3112(w), 2923(w), 1762(m), 1706(vs),

1613(s), 1563(s), 1402(s), 1371(vs), 1110(w), 1023(m), 788(m), 720(m), 634(w).

Synthesis of [Pb(HL)(DMSO)₂]·DMSO (2)

H₃L (3.5 mg, 0.01 mmol) and Pb(Ac)₂·3H₂O (11.9 mg, 0.04 mmol) were dissolved in a solvent mixture of DMSO/DMF(9.5:1, 2.0 mL) in a 20 ml scintillation vial, which was heated to 105 °C for 48 h, then cooled to room temperature. The colorless block crystals were collected by filtration, washed with DMSO and dried in air (52% yield based on H₃L). Element analysis (%) calcd for C₂₃H₂₅N₃O₉S₃Pb: C 34.93, H 3.18, N 5.31; found: C 34.52, H 2.98, N 5.27. IR (KBr pellet, cm⁻¹): 3411(br), 3115(w), 2924(w), 2846(w), 1766(s), 1707(vs), 1611(s), 1559(vs), 1416(s), 1371(vs), 1112(m), 1002(m), 931(m), 782(m), 720(m), 636(w).

Synthesis of [Mg(HL)(HCOOH)_{0.27}(DMSO)_{1.73}]·DMSO (3)

H₃L (3.5 mg, 0.01 mmol) and Mg(NO₃)₂ (2.2 mg, 0.015 mmol) were dissolved in a solvent mixture of DMSO/DMF/H₂O(10:6:1, 1.7 mL) in a 20 ml scintillation vial, which was heated to 105 °C for 48 h and cooled to room temperature. The colorless block crystals were collected by filtration, washed with DMSO and dried in air (48% yield based on H₃L). Element analysis (%) calcd for C_{22.73}H_{23.92}MgN₃O_{9.27}S_{2.73}: C 45.55, H 4.02, N 7.01; found: C 45.13, H 4.09, N 6.74. IR (KBr pellet, cm⁻¹): 3386(br), 2922(w), 1771(w), 1711(vs), 1633(s), 1578(s), 1422(s), 1376(vs), 1103(w), 1015(w), 783(m), 734(m), 640(m).

X-ray Structure Determinations

Intensity data of **1** and **1'** (150 K), and **2** (296 K) was measured on a Bruker SMART APEX II CCD area detector system. Data reduction and unit cell refinement were performed with Smart-CCD software. Data **3** was measured at 153 (2) K on a Mar CCD 165 mm detector by ω-scan techniques on the beamline 3W1A of BSRF (Beijing Synchrotron Radiation Facility) and the wavelength is 0.80000 Å. Data were corrected for absorption effects using the spherical harmonics technique. All the structures were solved by direct method using SHELXS-2014¹ and refined by full-matrix least squares method using SHELXS-2014¹. The hydrogen atoms were included in the structural model as fixed atoms (using idealized sp²-hybridized geometry and C-H bond lengths of 0.95Å) "riding" on their respective carbon atoms. No attempts were made to locate the hydrogen atoms on the carboxylate group of coordinated HCOOH of **3**. For **3**, coordinated HCOOH and one coordinated

DMSO molecule are partly occupied with occupy factors of 0.27 and 0.73 respectively. Large R₁ values for **3** may be caused by the part occupation and poor quality of the single crystal. A summary of the most important crystal and structure refinement data is given in Table S1. Selected bond lengths and angles of the compounds are given in Table S2-S4.

CCDC 2239223-2239226 contains the supplementary crystallographic data for this paper. These data can be obtained free of charge via www.ccdc.cam.ac.uk/conts/retrieving.html (or from the Cambridge Crystallographic Data Centre, 12 Union Road, Cambridge CB2 1EZ, UK; fax: (+44) 1223-336-033; or e-mail: deposit@ccdc.cam.ac.uk).

Periodic structure calculations through Material Studio software package

All calculations were performed with the periodic density functional theory (DFT) method using Dmol3 module in Material Studio software package². The initial configuration was fully optimized by Perdew-Wang (PW91) generalized gradient approximation (GGA) method with the double numerical basis sets plus polarization function (DNP)³⁻⁵. The core electrons for metals were treated by effective core potentials (ECP). The self-consistent field (SCF) converged criterion was within 1.0×10^{-5} hartree atom⁻¹ and the converging criterion of the structure optimization was 1.0×10^{-3} hartree bohr⁻¹. The Brillouin zone is sampled by $1 \times 1 \times 1$ k-points.

Excited state calculations through Gaussian software package

The energy bands and electronic structures of **1**, **1-DMSO** (the uncoordinated DMSO molecule in **1** is lost), and **1-DMSO-H₂O** (one of the coordination DMSO molecules in **1-DMSO** is replaced by a H₂O molecule), periodical density functional theoretical (PDFT) using Material Studio package were performed on their crystal models. In order to understand the photophysical properties in depth, asymmetry units [Ca(HL)H·(DMSO)₂] (**1-DMSO-F**) and [Ca(HL)·DMSO·H₂O] (**1-DMSO-H₂O-F**) were extracted from the optimized periodic structures of **1-DMSO** and **1-DMSO-H₂O**, and used to simulate the two models, respectively. The singlet and triplet states of both the **1-DMSO-F** and **1-DMSO-H₂O-F** were optimized at the wB97XD level of theory⁶ and the def2-svp basis set⁷ based on the Gaussian 16 package.⁸ Single point energy was further calculated based on the ma-def2-TZVP(-f) basis set^{9,10}. DFT-D3 dispersion correction method provides corrections to the energy¹¹. The analyses of HOMO and LUMO were performed in the Multiwfn program¹² and visualized through the Visual Molecular Dynamics software¹³.

Table S1. Crystallographic data for complexes **1**- **3**.

	1	1'	2	3
Formula	C ₂₃ H ₂₅ N ₃ O ₉ CaS ₃	C ₂₃ H ₂₅ N ₃ O ₉ CaS ₃	C ₂₃ H ₂₅ PbN ₃ O ₉ S ₃	C _{22.73} H _{23.92} MgN ₃ O _{9.27} S _{2.73}
Formula weight	623.72	623.72	790.83	599.29
Crystal system	Triclinic	triclinic	Triclinic	Triclinic
Space group	P-1	P-1	P-1	P-1
<i>a</i> (Å)	8.2621(6)	8.2656(5)	8.6284(4)	8.4250(17)
<i>b</i> (Å)	10.1118(6)	10.1091(5)	10.1963(4)	10.096(2)
<i>c</i> (Å)	16.0255(12)	16.0219(9)	16.2383(7)	15.873(3)
α (°)	85.357(2)	85.342(2)	85.516(3)	96.99(3)
β (°)	89.946(3)	89.964(2)	89.733(4)	93.113(3)
γ (°)	76.629(2)	76.626(2)	78.473(3)	92.64(3)
<i>V</i> (Å ³)/ <i>Z</i>	1298.06(16)/2	1297.92(13)/2	1395.42(10)/2	1336.2(5)/2
<i>D_{calcd}</i> (g /cm ³)	1.596	1.596	1.882	1.489
μ (mm ⁻¹)	0.542	0.542	6.325	0.337
<i>F</i> (000)	648	648	772	622
θ range(°)	2.07 -25.00	2.35-25.00	2.04-25.00	2.27 -29.54
Reflections	31762 / 4564	58689 / 4571	7203 / 4846	6669 / 6669
collected / unique				
<i>R</i> (int)	0.0607	0.0599	0.0226	0.0000
GOF on F ²	1.096	1.042	1.049	0.991
<i>R₁</i> ^a , <i>I</i> >2σ(<i>I</i>) (all)	0.0462 (0.1141)	0.0387(0.0505)	0.0282 (0.0658)	0.0940 (0.2184)
<i>wR₂</i> ^b , <i>I</i> >2σ(<i>I</i>) (all)	0.0583 (0.1209)	0.1005(0.1055)	0.0329 (0.0673)	0.0982 (0.2209)
Max/mean shift in final cycle	0.001/0.000	0.001/0.000	0.001/0.000	0.000/0.000

^a*R*= $\sum(|F_o|-|F_c|)/\sum|F_o|$, ^b*Rw*= $\{\sum w[(F_o^2-F_c^2)]/\sum w[(F_o^2)^2]\}^{0.5}$, *w* = [$\sigma^2(F_o^2) + (aP)^2+bP$] $^{-1}$, where *P* = (*F_o²* + 2 *F_c²*)/3.]. **1**, *a* = 0.0585, *b* = 0.9579; **1'**, *a* = 0.0536, *b* = 1.4970; **2**, *a* = 0.0363, *b* = 0.3551; **3**, *a* = 0.0562, *b* = 11.8634.

Table S2. Selected bond lengths (Å) and angles (°) for **1** and **1'**.

1		1'	
Ca(1)-O(7)	2.295(2)	Ca(1)-O(7)	2.297(2)
Ca(1)-O(4)#1	2.305(2)	Ca(1)-O(4)#1	2.305(2)
Ca(1)-O(8)	2.339(2)	Ca(1)-O(8)	2.341(2)
Ca(1)-O(3)#2	2.402(2)	Ca(1)-O(3)#2	2.403(2)
Ca(1)-O(1)	2.429(2)	Ca(1)-O(1)	2.429(2)
Ca(1)-O(4)#2	2.661(2)	Ca(1)-O(4)#2	2.660(2)
Ca(1)-O(2)	2.422(2)	Ca(1)-O(2)	2.420(2)
O(7)-Ca(1)-O(4)#1	85.02(8)	O(7)-Ca(1)-O(4)#1	85.16(7)
O(7)-Ca(1)-O(8)	172.13(8)	O(7)-Ca(1)-O(8)	172.25(7)
O(4)#1-Ca(1)-O(8)	88.94(8)	O(4)#1-Ca(1)-O(8)	88.86(7)
O(7)-Ca(1)-O(3)#2	93.32(8)	O(7)-Ca(1)-O(3)#2	93.21(7)
O(4)#1-Ca(1)-O(3)#2	128.02(7)	O(4)#1-Ca(1)-O(3)#2	127.92(6)
O(8)-Ca(1)-O(3)#2	94.38(8)	O(8)-Ca(1)-O(3)#2	94.36(7)

O(7)-Ca(1)-O(2)	87.99(9)	O(7)-Ca(1)-O(2)	87.90(8)
O(4)#1-Ca(1)-O(2)	99.90(7)	O(4)#1-Ca(1)-O(2)	99.91(6)
O(8)-Ca(1)-O(2)	88.08(9)	O(8)-Ca(1)-O(2)	88.26(8)
O(3)#2-Ca(1)-O(2)	132.01(7)	O(3)#2-Ca(1)-O(2)	132.10(6)
O(7)-Ca(1)-O(1)	92.68(9)	O(7)-Ca(1)-O(1)	92.62(7)
O(4)#1-Ca(1)-O(1)	154.26(7)	O(4)#1-Ca(1)-O(1)	154.36(6)
O(8)-Ca(1)-O(1)	90.57(8)	O(8)-Ca(1)-O(1)	90.63(7)
O(3)#2-Ca(1)-O(1)	77.67(7)	O(3)#2-Ca(1)-O(1)	77.68(6)
O(2)-Ca(1)-O(1)	54.36(7)	O(2)-Ca(1)-O(1)	54.45(6)
O(7)-Ca(1)-O(4)#2	98.73(8)	O(7)-Ca(1)-O(4)#2	98.66(7)
O(4)#1-Ca(1)-O(4)#2	77.68(7)	O(4)#1-Ca(1)-O(4)#2	77.60(6)
O(8)-Ca(1)-O(4)#2	84.86(7)	O(8)-Ca(1)-O(4)#2	84.84(7)
O(3)#2-Ca(1)-O(4)#2	51.17(7)	O(3)#2-Ca(1)-O(4)#2	51.14(6)
O(2)-Ca(1)-O(4)#2	172.57(8)	O(2)-Ca(1)-O(4)#2	172.70(7)
O(1)-Ca(1)-O(4)#2	127.90(7)	O(1)-Ca(1)-O(4)#2	127.88(6)
Ca(1)#1-O(4)-Ca(1)#4	102.32(7)	Ca(1)#1-O(4)-Ca(1)#4	102.40(6)

Symmetry transformations used to generate equivalent atoms: #1 -x+2, -y, -z+2; #2 x, y-1, z; #3 -x+2, -y-1, -z+2; #4 x, y+1, z.

Table S3. Selected bond lengths (Å) and angles (°) for **2**.

Pb(1)-O(3)#1	2.449(3)	Pb(1)-O(14)	2.594(5)
Pb(1)-O(13)	2.466(5)	Pb(1)-O(4)#2	2.745(4)
Pb(1)-O(1)	2.516(3)	O(3)-Pb(1)#3	2.449(3)
Pb(1)-O(2)	2.536(4)	O(4)-Pb(1)#2	2.745(4)
O(3)#1-Pb(1)-O(13)	90.18(16)	O(1)-Pb(1)-O(14)	85.29(16)
O(3)#1-Pb(1)-O(1)	76.14(10)	O(2)-Pb(1)-O(14)	90.9(2)
O(13)-Pb(1)-O(1)	93.9(2)	O(3)#1-Pb(1)-O(4)#2	127.80(10)
O(3)#1-Pb(1)-O(2)	126.70(13)	O(13)-Pb(1)-O(4)#2	86.50(19)
O(13)-Pb(1)-O(2)	84.9(2)	O(1)-Pb(1)-O(4)#2	156.06(11)
O(1)-Pb(1)-O(2)	51.47(12)	O(2)-Pb(1)-O(4)#2	104.87(12)
O(3)#1-Pb(1)-O(14)	94.23(15)	O(14)-Pb(1)-O(4)#2	92.27(16)
O(13)-Pb(1)-O(14)	175.21(17)		

Symmetry transformations used to generate equivalent atoms: #1 x, y-1, z; #2 -x+2, -y+1, -z+1; #3 x, y+1, z.

Table S4. Selected bond lengths (Å) and angles (°) for **3**.

Mg(1)-O(3)#1	1.995(3)	Mg(1)-O(2)	2.139(3)
Mg(1)-O(4)#2	2.022(3)	Mg(1)-O(1)	2.198(3)
Mg(1)-O(9)	2.062(4)	O(3)-Mg(1)#1	1.995(3)
Mg(1)-O(8')	2.098(4)	O(4)-Mg(1)#3	2.022(3)
O(3)#1-Mg(1)-O(4)#2	112.02(12)	O(9)-Mg(1)-O(2)	90.25(13)
O(3)#1-Mg(1)-O(9)	92.98(15)	O(8')-Mg(1)-O(2)	88.25(13)
O(4)#2-Mg(1)-O(9)	89.74(13)	O(3)#1-Mg(1)-O(1)	152.25(12)
O(3)#1-Mg(1)-O(8')	91.80(15)	O(4)#2-Mg(1)-O(1)	95.61(11)
O(4)#2-Mg(1)-O(8')	89.76(13)	O(9)-Mg(1)-O(1)	89.60(13)

O(9)-Mg(1)-O(8')	175.03(14)	O(8')-Mg(1)-O(1)	85.53(13)
O(3)#1-Mg(1)-O(2)	91.39(12)	O(2)-Mg(1)-O(1)	60.95(10)
O(4)#2-Mg(1)-O(2)	156.56(13)		

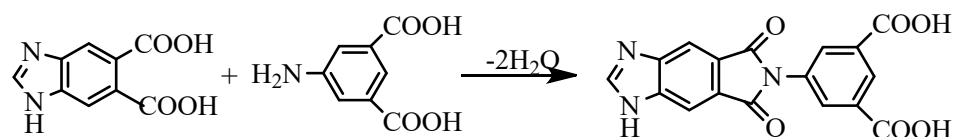
Symmetry transformations used to generate equivalent atoms: #1 -x, -y+1, -z; #2 x, y-1, z; #3 x, y+1, z.

Table S5. The phosphorescence lifetime (τ) of different compounds.

λ_{em} (nm)	τ			
	τ_1/ms	τ_2/ms	τ_3/ms	$\tau_{\text{av}}/\text{ms}$
H ₃ L	488	1.5(12.553)	6.6(34.977)	27(52.470)
1	463	5.6(11.015)	27(37.351)	87(51.634)
2	503	6.6(1.643)	35(33.770)	76(64.587)
3	497	4(9.540)	15(25.294)	48(65.166)
1-H	503	0.28(22.143)	1.6(43.549)	7.2(34.308)
				3.2

Table S6. A comparison of the luminescence data of **1** before and after solvent exchange.

	λ_{em} (nm)	τ (ms)	QY (%)
1	463	55.6	3.54
1-H	503	3.2	3.53



Scheme S1. Synthesis of the H_3L ligand.

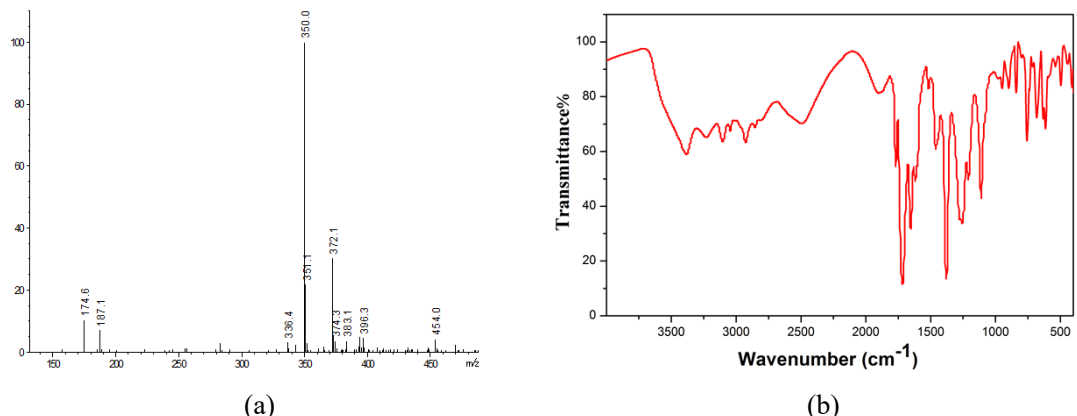


Figure S1. Electrospray ionization (a) and IR (b) spectra of the H_3L ligand.

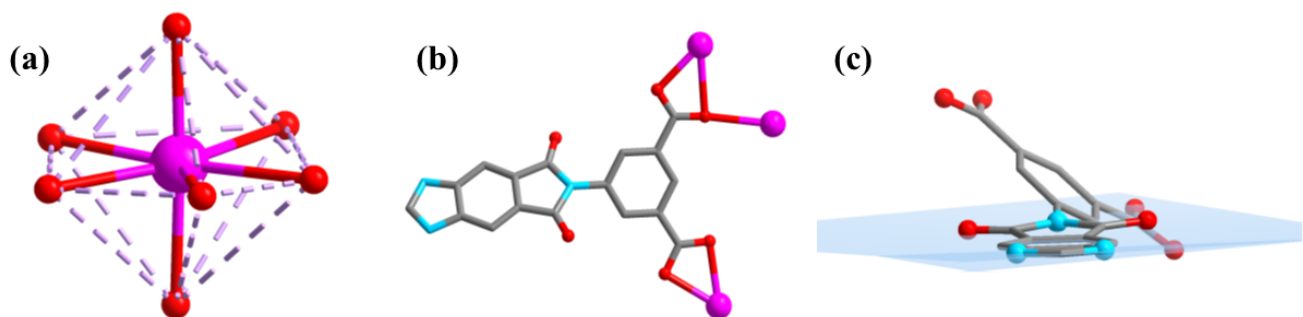


Figure S2. The structure of **1**. (a) The coordination environment of the Ca^{2+} ion in **1**; (b) The bridging mode of the HL^{2-} ligand in **1**; (c) The configuration of the HL^{2-} ligand in **1**.

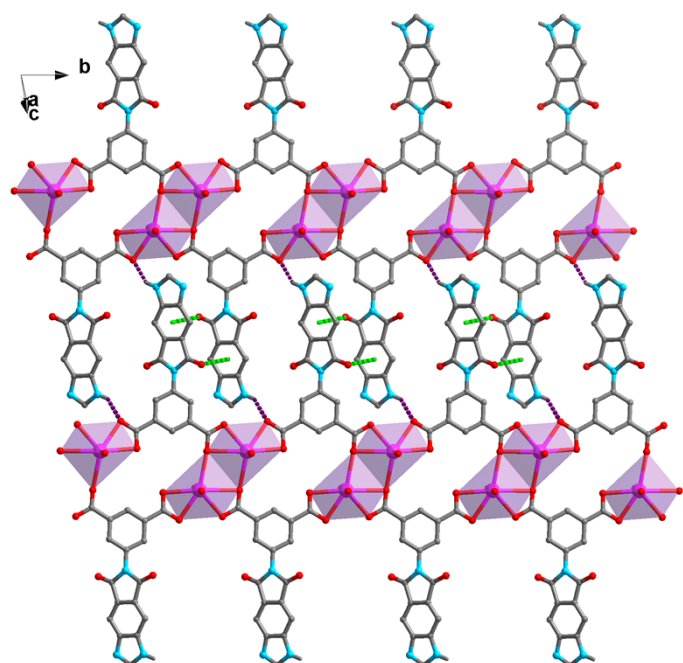


Figure S3. One 2D layer formed through weak interactions in **1**. Inter-belt $\pi\text{-}\pi$ interactions and hydrogen bonds are represented as dotted green and purple lines respectively.

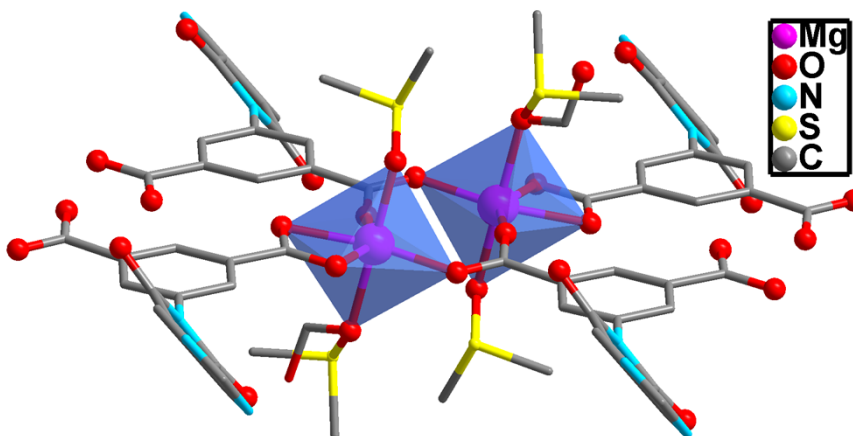


Figure S4. The coordination environment of the binuclear Mg^{2+} center in **3**.

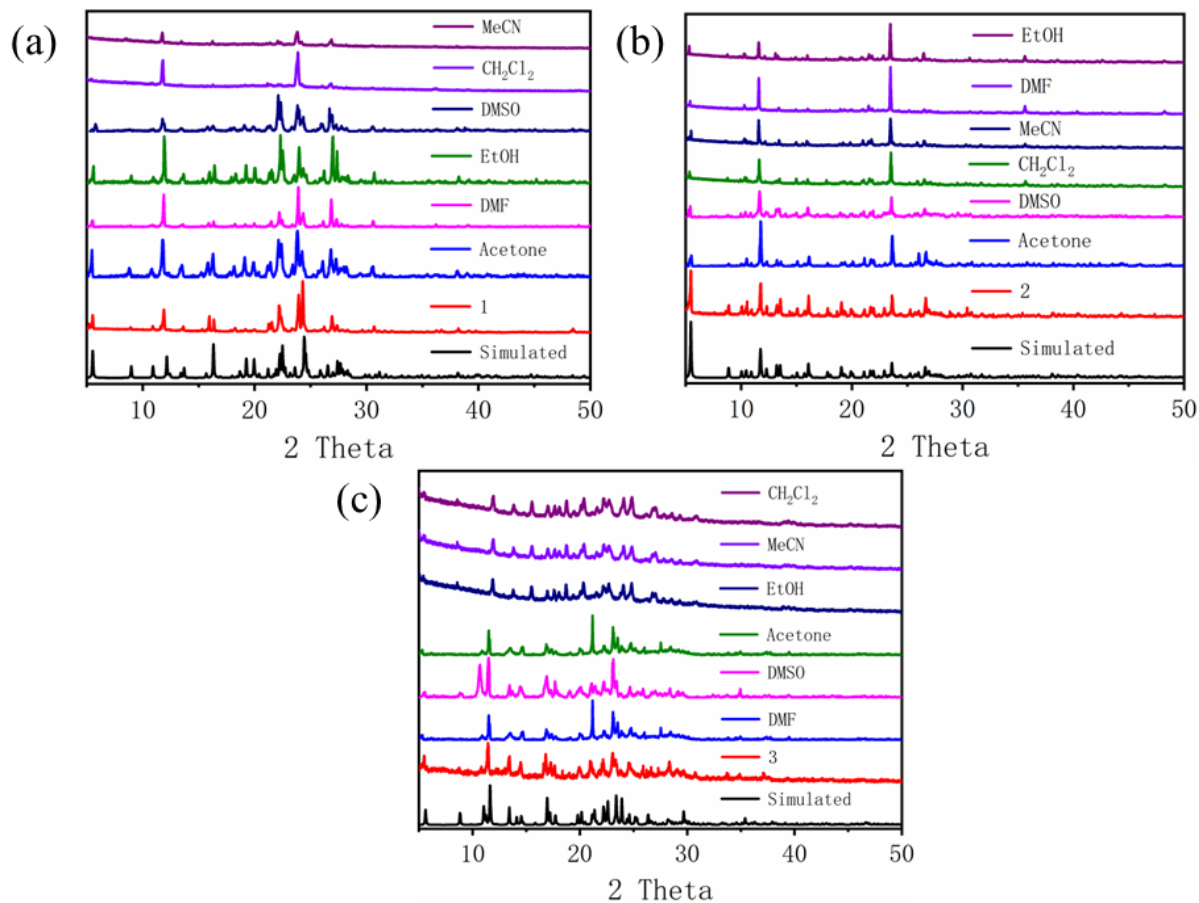


Figure S5. PXRD results. (a) Experimental and simulated PXRD patterns of **1**, and **1** being soaked in different solvents for 1h. (b) Experimental and simulated PXRD patterns of **2**, and **2** being soaked in different solvents for 1h. (c) Experimental and simulated PXRD patterns of **3**, and **3** being soaked in different solvents for 1h.

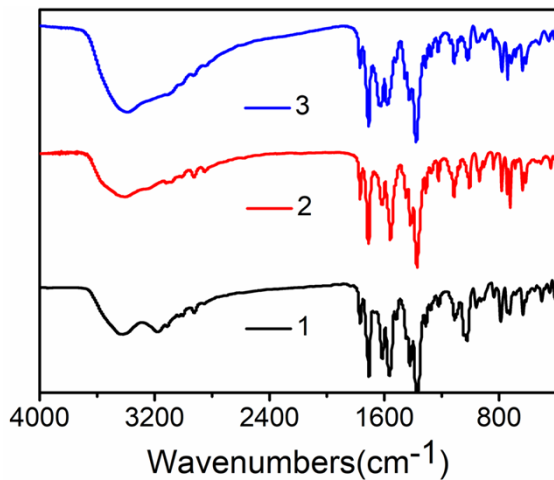


Figure S6. IR spectra of compounds **1-3**.

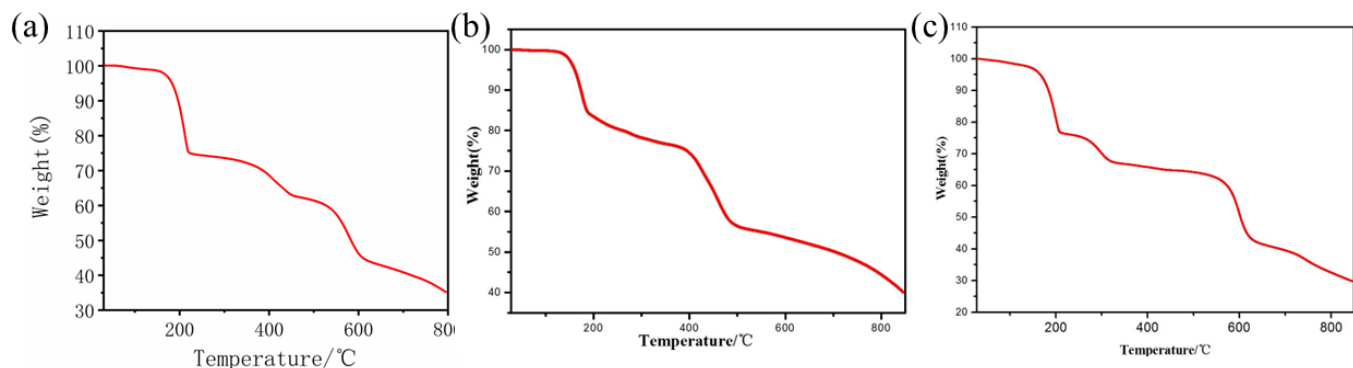


Figure S7. TGA curves of the compounds (a) **1**, (b) **2** and (c) **3**.

2 is stable before 130°C and lost its 24.63% weight at 130–383 °C, corresponding to the loss of 2.5 DMSO molecules (cal. 24.70%). After 383 °C, the material continuous lost its weight until 850 °C. Curve of **3** exhibits three distinct weight losses. The first step (23.31 %) involves the loss of 2 DMSO solvent molecules in the temperature region of 30-209 °C (cal. 26.07 %). **3** lost the remaining 0.73 DMSO and 0.27 HCOOH molecules (% loss (obs.) =13.15%; %loss (calc.) = 11.59%) in the second step (209-500°C). After 500°C, the material shows a striking weight loss, indicating the completed decomposition of the structure.

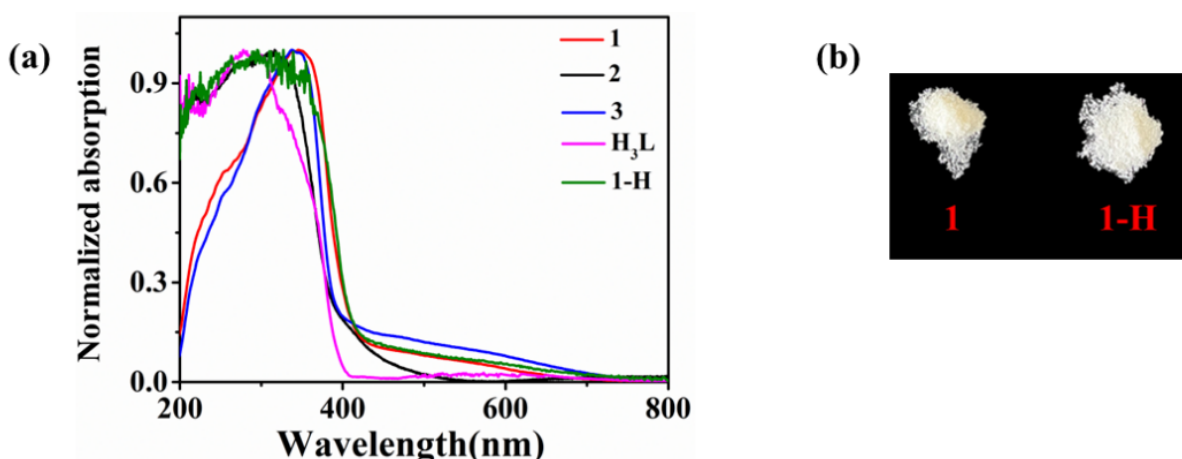


Figure S8. (a) The UV-Vis diffuse reflectance spectra of H_3L , **1-H** and **1-3**. (b) The photos of **1** and **1-H** under sunlight.

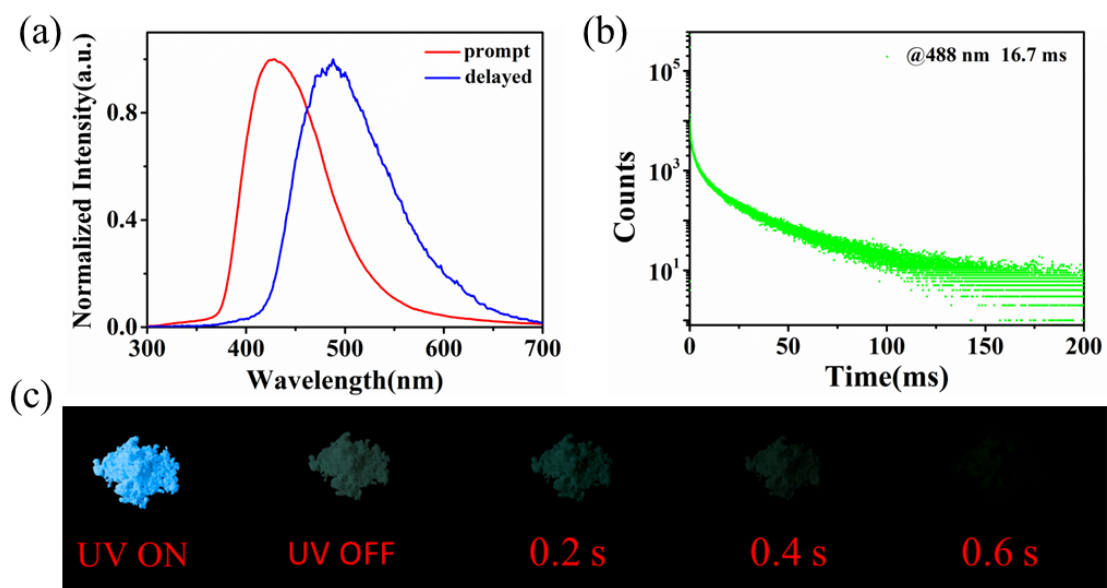


Figure S9. Luminescence properties of the ligand. (a) Normalized prompt (red line) and delayed spectra (blue line). (b) Time-resolved emission decay curve (the excitation and emission wavelengths are 254 and 488 nm, respectively) under ambient conditions. (c) Photographs before and after turning off the 254 nm UV lamp.

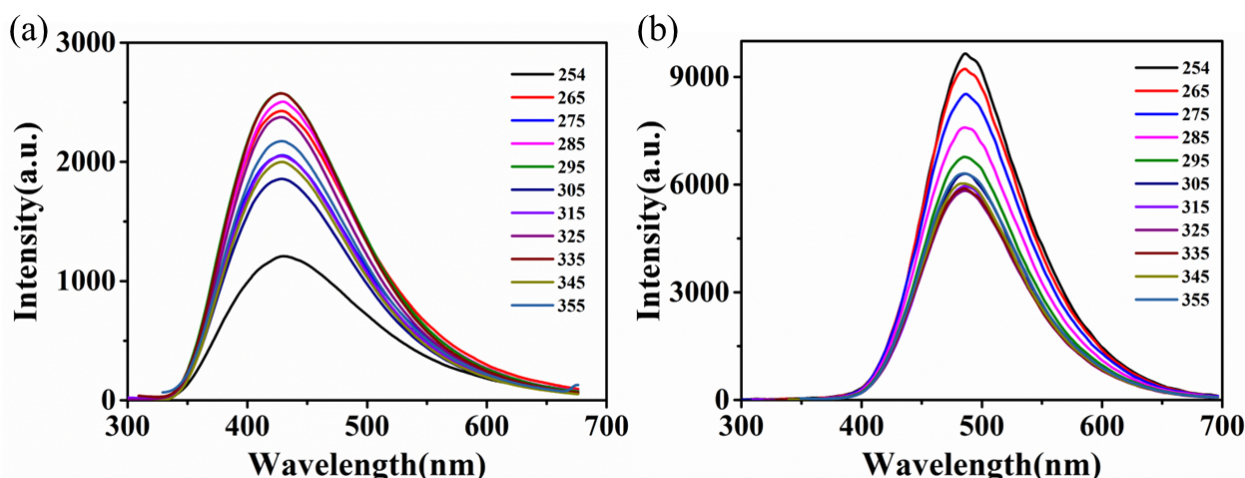


Figure S10. The solid state emission spectra of the ligand under different excitation wavelength. (a) Prompt spectra. (b) Delayed spectra .

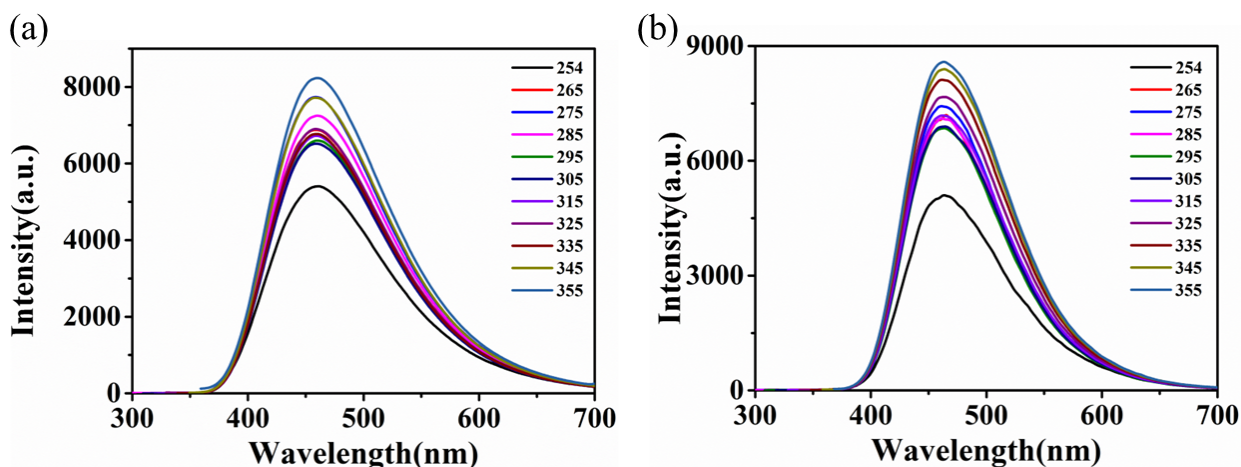


Figure S11. The solid state emission spectra of **1** under different excitation wavelength. (a) Prompt spectra. (b) Delayed spectra .

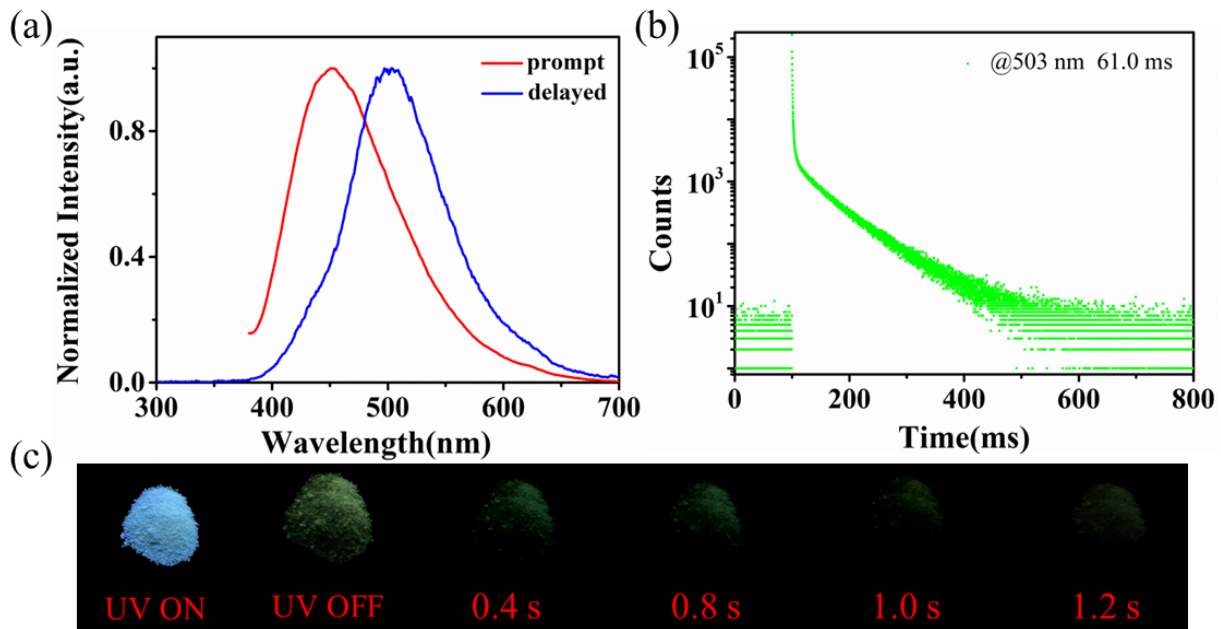


Figure S12. Luminescence properties of **2**. (a) Normalized prompt (red line) and delayed photoluminescence spectra (blue line). (b) Time-resolved emission decay curve ($\lambda_{\text{ex}} = 254$ nm and the emission wavelength is 503 nm) under ambient conditions. (c) Photographs before and after turning off the UV excitation.

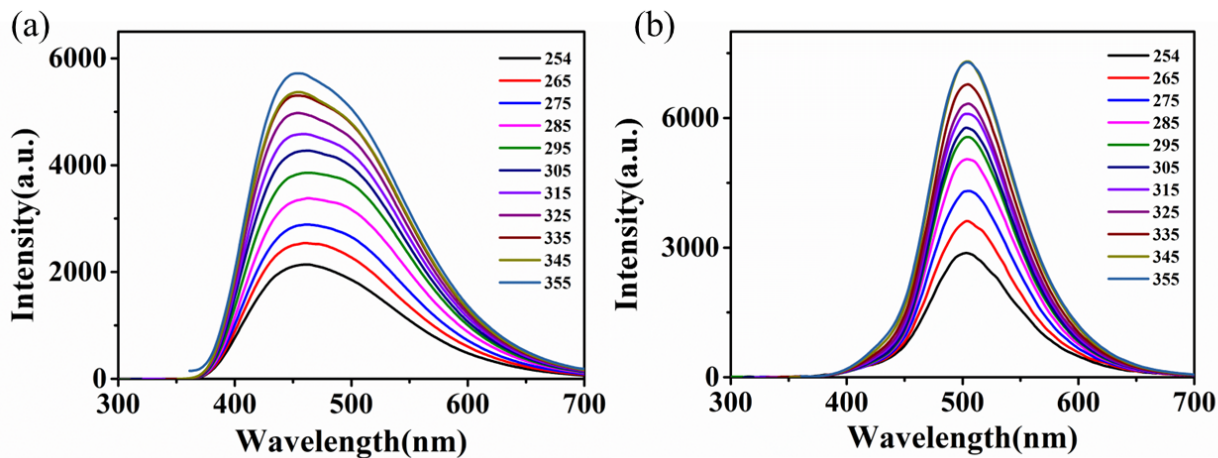


Figure S13. The solid state emission spectra of **2** under different excitation wavelength. (a) Prompt spectra. (b) Delayed spectra .

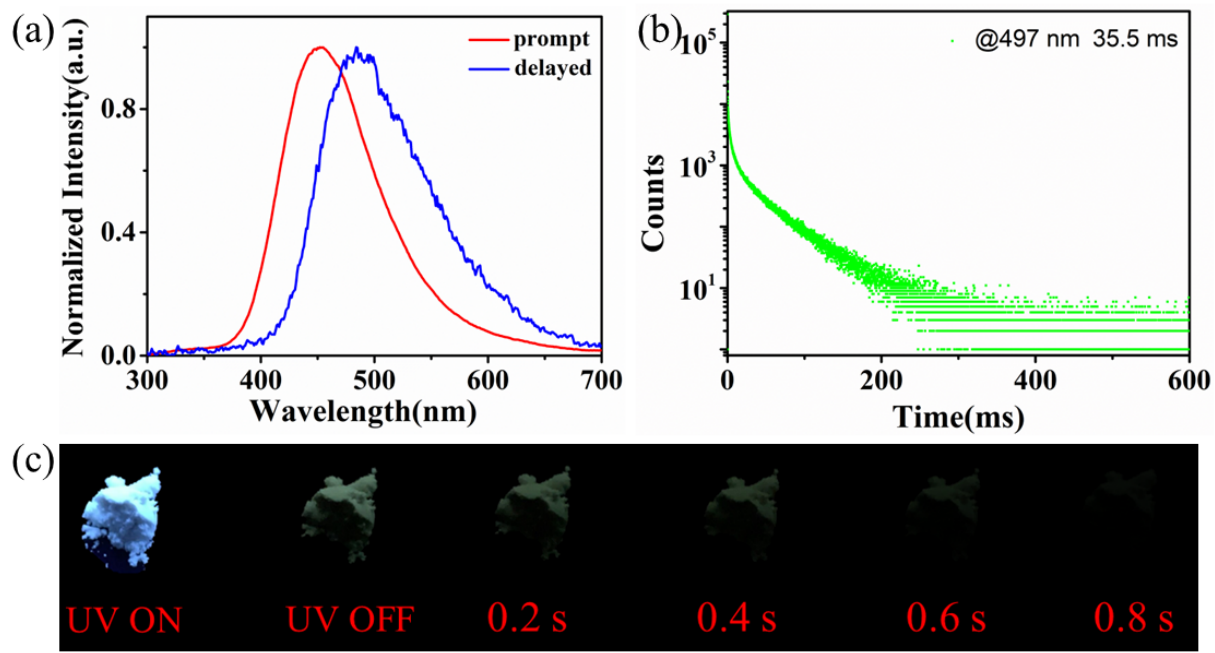


Figure S14. Luminescence properties of **3**. (a) Normalized prompt (red line) and delayed (blue line) photoluminescence spectra. (b) Time-resolved emission decay curves ($\lambda_{\text{ex}} = 254$ nm and the emission wavelength is 497 nm) under ambient conditions. (c) Photographs before and after turning off the UV excitation.

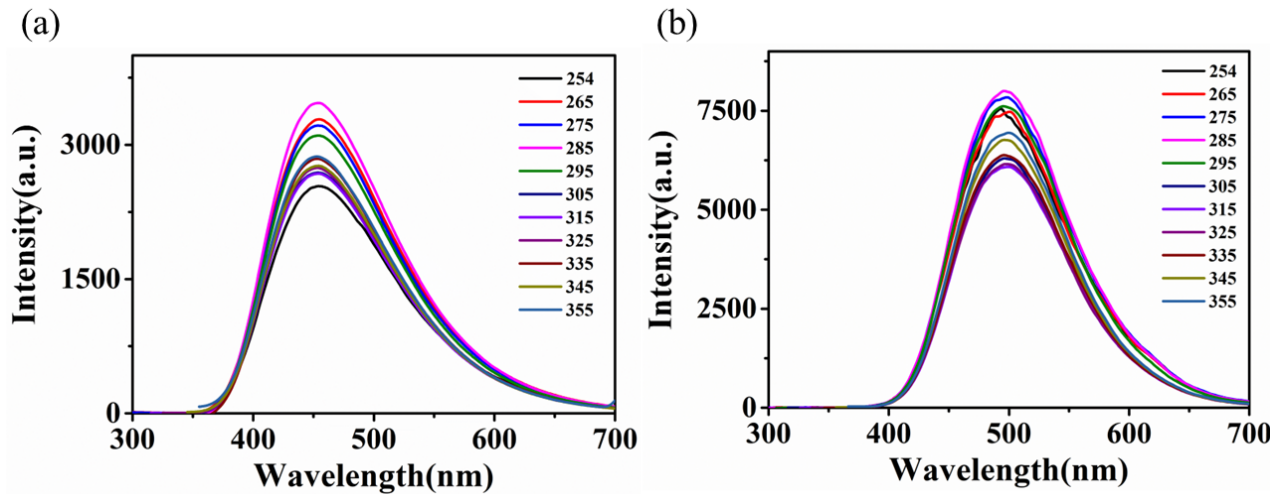


Figure S15. The solid state emission spectra of **3** under different excitation wavelength. (a) Prompt spectra. (b) Delayed spectra .

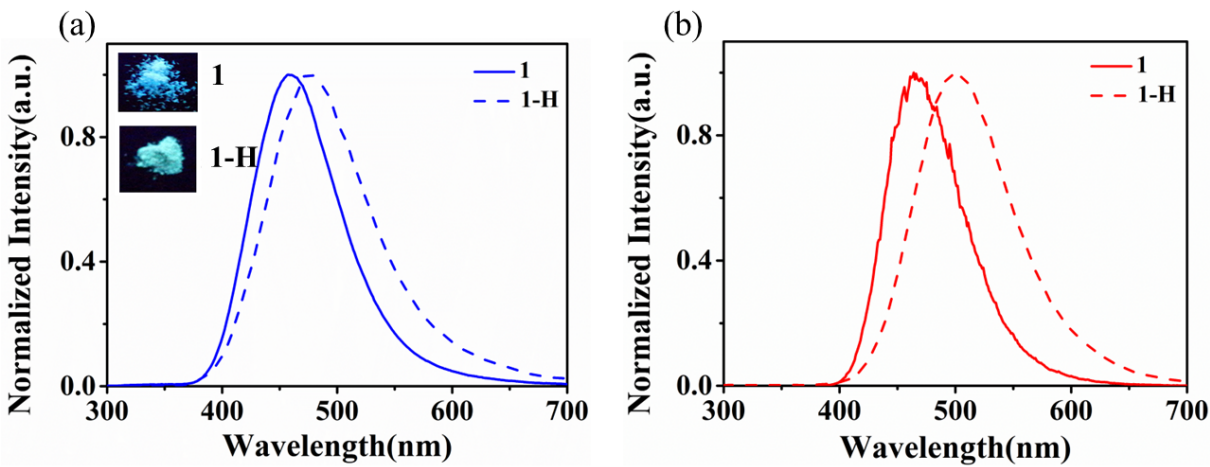


Figure S16. A comparison of luminescence spectra of initial **1** and **1** exposed to air for three hours (**1-H**). (a) Normalized prompt spectra. (b) Normalized delayed spectra.

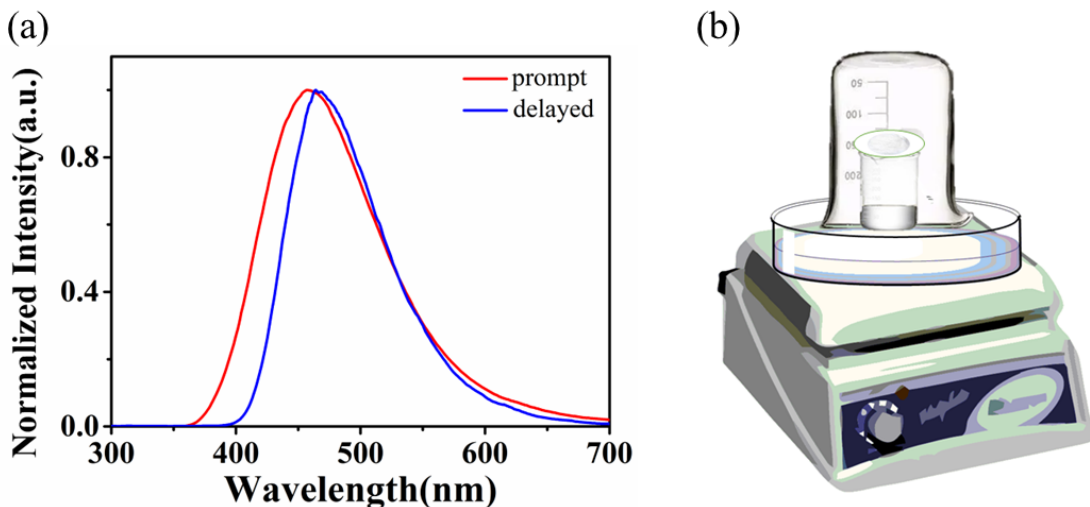


Figure S17. (a) Normalized prompt (red line) and delayed (blue line) emission spectra of **1** heated at 120°C for 20min. (b) Installation diagram.

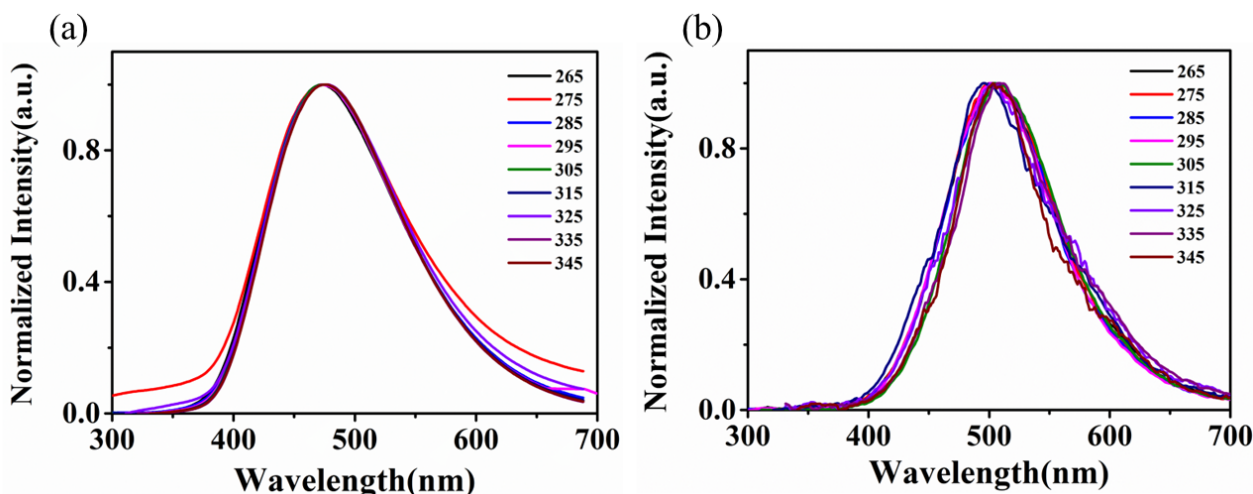


Figure S18. The solid state emission spectra of **1-H** under different excitation wavelength. (a) Prompt spectra. (b) Delayed

spectra .

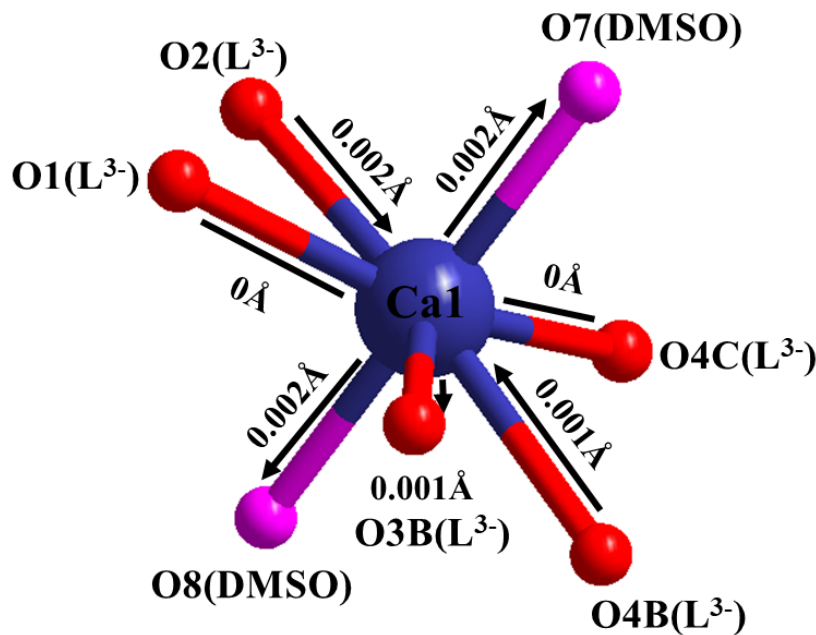


Figure S19. Illustration of changes in Ca–O bond lengths of compounds **1** and **1'**.

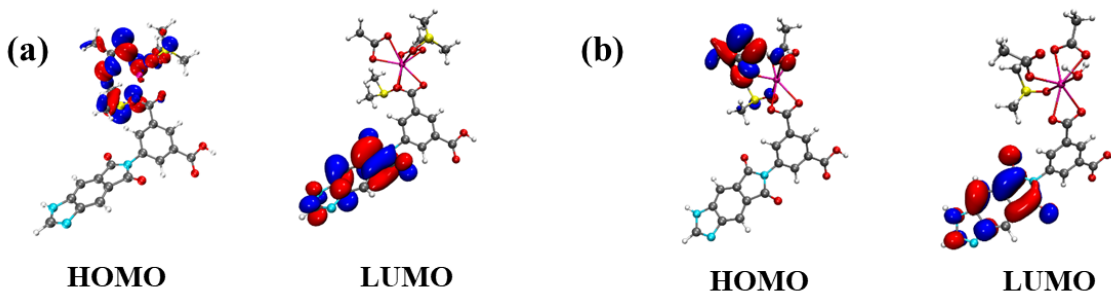


Figure S20. (a) HOMO and LUMO distribution of **1**-DMSO-F.(b) HOMO and LUMO distribution of **1**-DMSO-H₂O-F.

The related geometry data for **1**-DMSO-F:

O	2.78294130	5.47426043	-1.67325819
C	1.74392523	4.93472839	-1.37519417
Ca	-3.40350215	-0.49427400	0.17043594
S	-4.45662523	1.51668115	2.89151314
S	-1.83474004	-1.94412910	-2.68327126
C	-0.68040496	-2.69232516	-1.50815418
H	0.11619110	-1.95635111	-1.33950816
H	-0.27248393	-3.61011122	-1.95757221
C	-3.13242913	-3.20350219	-2.60720926
H	-2.81616211	-4.07119926	-3.20516230
H	-4.03318620	-2.72859316	-3.01735329
H	-3.31230015	-3.45192421	-1.55005018
H	-1.22025000	-2.89443517	-0.57104211
O	-4.88269826	-2.02261911	1.54959604

O	-3.15113314	-2.90419217	0.48509697
O	-0.99523098	-0.20645598	0.53993897
O	-2.06552505	1.64309316	-0.09024008
O	3.29943833	-1.17434105	-1.21084516
O	5.15782247	2.25027519	1.22342602
O	-3.45030915	0.52749808	2.34477210
O	-2.38765708	-0.70548201	-2.00992221
N	8.29682271	-3.28586321	0.24022395
H	8.20842868	-4.19254328	-0.19606008
N	9.21387974	-1.61905909	1.41387503
N	3.91118838	0.74144808	-0.03489207
C	9.37048874	-2.82537218	0.95529200
H	10.25625785	-3.44428522	1.10383801
C	7.35736662	-2.28086814	0.23835295
C	7.95830067	-1.23492707	0.98755900
C	6.07930455	-2.18983013	-0.32815209
H	5.60720547	-2.98739619	-0.90401413
C	7.27503161	-0.02545398	1.20287002
H	7.71320466	0.79204008	1.77631706
C	5.44141646	-0.98939804	-0.09552708
C	6.01627652	0.05600603	0.64384498
C	4.08447339	-0.55478701	-0.54492811
C	5.03425246	1.18198712	0.68856598
C	2.72130929	1.50591914	-0.21587809
C	2.79688830	2.81195523	-0.68903812
H	3.75488537	3.28032927	-0.91552313
C	1.61776021	3.54309429	-0.86841513
C	0.37639913	2.95933824	-0.59601011
H	-0.55884394	3.49922828	-0.74839712
C	0.30942912	1.64864515	-0.12816308
C	1.48452020	0.92958210	0.07437594
H	1.39548319	-0.09096497	0.44977096
C	-4.22205921	-3.00025018	1.15310001
C	-1.03374898	0.97859311	0.13934794
C	-4.61348823	2.82103024	1.64547105
H	-5.01777826	2.38080021	0.72142498
H	-3.59105916	3.17808927	1.46353103
H	-5.25347028	3.62120130	2.04633608
C	-6.08617634	0.75527110	2.68735212

H	-6.25706233	0.59738108	1.61158105
H	-6.84408342	1.40688014	3.14727316
O	-5.48643330	0.64587709	-0.37146210
O	-5.29130528	-1.28305205	-1.44352118
C	-7.35638743	-0.09429496	-1.65060619
C	-5.93057336	-0.26399898	-1.13425815
C	-4.74817925	-4.40540028	1.42658803
H	-6.02865932	-0.21718597	3.19309816
H	-5.31230727	-4.73618230	0.53986597
H	-5.42693129	-4.40799027	2.28991910
H	-3.91762219	-5.10795933	1.58252804
H	-7.55017446	0.95710411	-1.90586021
H	-8.05325851	-0.37841698	-0.84593213
H	-7.53934543	-0.74277701	-2.51756925
O	0.56747415	5.57113844	-1.48222518
H	0.77072716	6.45177749	-1.82444220

The related geometry data for 1-DMSO-H₂O-F:

O	-2.57016540	5.68674166	0.92335315
C	-1.51842294	5.20709143	0.57381871
Ca	3.84361646	0.10133630	-0.47607788
S	2.21896128	-1.11997541	2.39849991
C	1.12085286	-2.01073424	1.27143917
H	0.25075073	-1.36791410	1.09380578
H	0.80832403	-2.94139016	1.76614789
C	3.57541210	-2.31531644	2.41793948
H	3.27695382	-3.18580468	3.02074919
H	4.43183513	-1.79327483	2.85716397
H	3.81297134	-2.57484062	1.37463457
H	1.66932125	-2.20349355	0.33690806
O	5.43707705	-2.51223718	-2.17812724
O	3.74222822	-2.22457675	-0.75100103
O	1.48561706	0.13125546	-1.10785271
O	2.44340776	2.08911761	-0.71110431
O	-2.49635955	-0.99108843	1.12621945
O	-4.91562705	1.99253727	-1.39828197

O	2.73940352	0.08862734	1.63754820
N	-7.38661551	-3.66059718	0.45590615
H	-7.16671326	-4.50469056	0.96551875
N	-8.57559487	-2.21375749	-0.76446137
N	-3.40945861	0.73441645	-0.14695392
C	-8.56730701	-3.37286590	-0.17638959
H	-9.39997582	-4.07723611	-0.16415494
C	-6.55304387	-2.58535283	0.25456130
C	-7.32695173	-1.68023213	-0.52022024
C	-5.24081272	-2.32224296	0.66394779
H	-4.63441462	-3.01111341	1.25660870
C	-6.79140610	-0.44599960	-0.92706786
H	-7.36465296	0.26404969	-1.52457767
C	-4.74929047	-1.10490319	0.24550346
C	-5.49629743	-0.19633438	-0.52211885
C	-3.40473919	-0.50987432	0.49845880
C	-4.63922226	1.00046291	-0.78195491
C	-2.28778895	1.61254235	-0.16297400
C	-2.43632880	2.94790478	0.19548904
H	-3.40727462	3.35679686	0.47643762
C	-1.31615492	3.78577936	0.18625639
C	-0.05696216	3.27952693	-0.15372537
H	0.83691315	3.90498751	-0.14276850
C	0.08081417	1.93875650	-0.50343771
C	-1.03723370	1.11288945	-0.52625582
H	-0.89374288	0.07125157	-0.81553400
C	4.65347278	-2.91239035	-1.29818542
C	1.44419729	1.34463164	-0.81635307
O	6.14811892	1.06422107	-0.44530899
O	5.73850593	-0.61765613	0.93183584
C	8.01936534	0.04835280	0.64272355
C	6.52376634	0.18088100	0.37278303
C	4.82404487	-4.33749859	-0.77955640

H	5.41562912	-4.29437868	0.14965643
H	5.35964191	-4.95849379	-1.50544515
H	3.84877631	-4.78171586	-0.53718750
H	8.51558517	1.02642410	0.56763900
H	8.44538346	-0.61253821	-0.12955024
H	8.19920448	-0.41058641	1.62396411
O	-0.39831550	5.94023645	0.50432897
H	-0.64274226	6.83386204	0.78027245
H	5.67767092	0.49717038	-2.28168025
H	5.14759120	-0.91946436	-2.63145530
O	4.91100365	0.04837110	-2.67299923

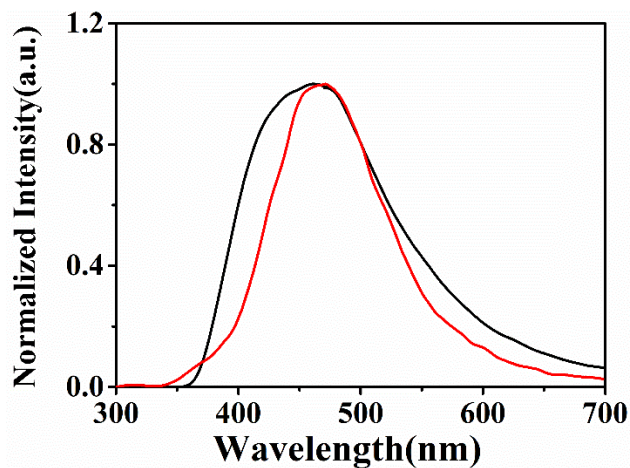


Figure S21. Normalized prompt (black line) and delayed (red line) emission spectra of **1** heated at 190°C for 20min.

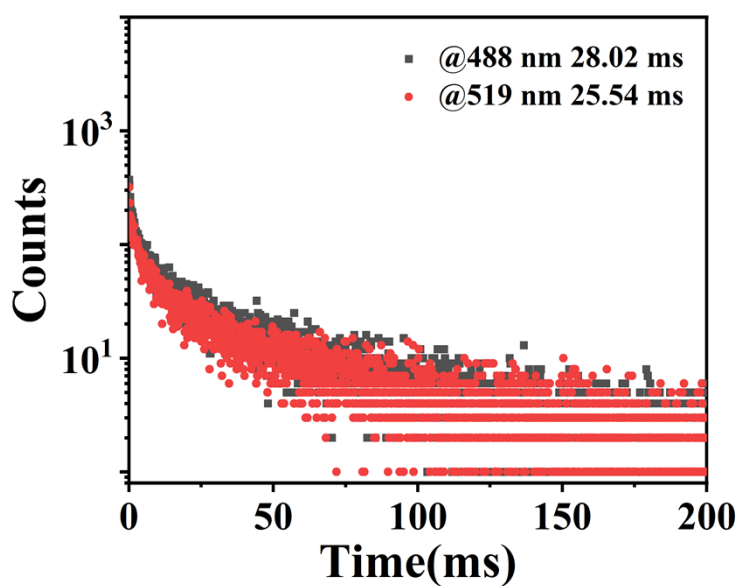


Figure S22. Time-resolved emission decay curves of **1** under ambient conditions.

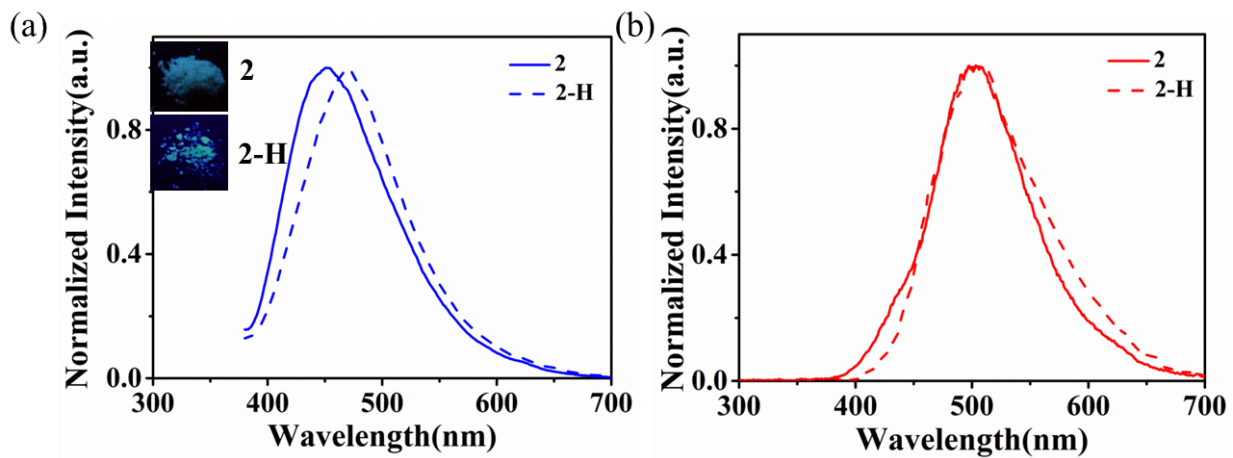


Figure S23. A comparison of luminescence spectra of initial **2** and **2** exposed to air for three hours (**2-H**). (a) Normalized prompt spectra. (b) Normalized delayed spectra.

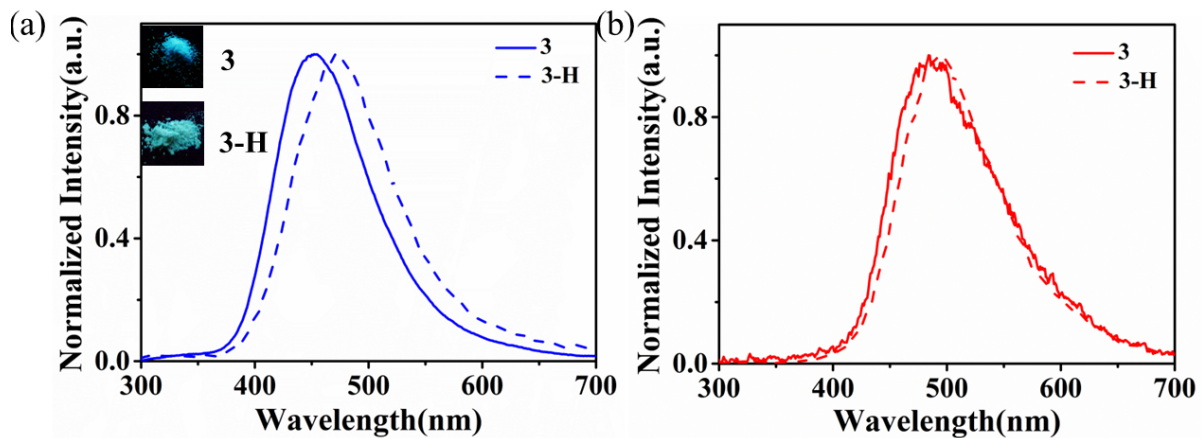


Figure S24. A comparison of luminescence spectra of initial **3** and **3** exposed to air for three hours (**3-H**). (a) Normalized prompt spectra. (b) Normalized delayed spectra.

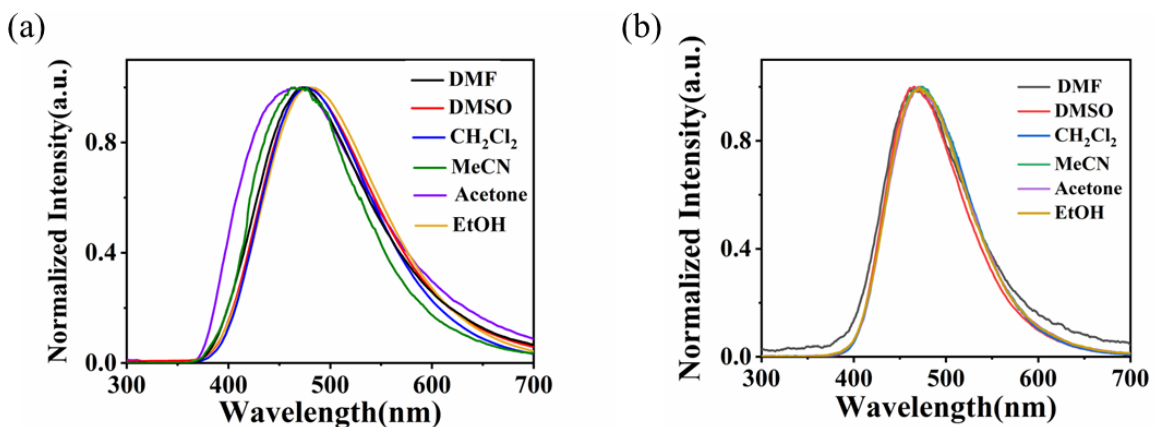


Figure S25. Normalized prompt (a) and delayed (b) emission spectra of **1** after soaked in different solvents.

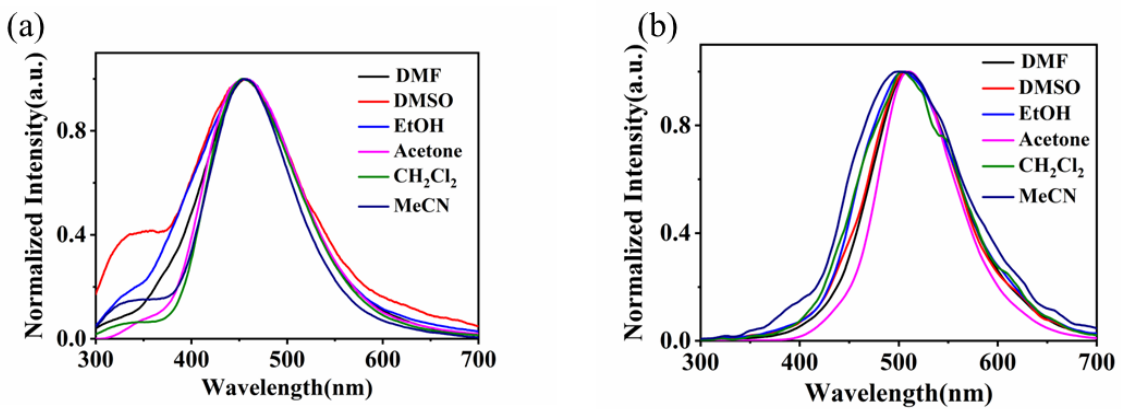


Figure S26. Normalized prompt (a) and delayed (b) emission spectra of **2** after soaked in different solvents.

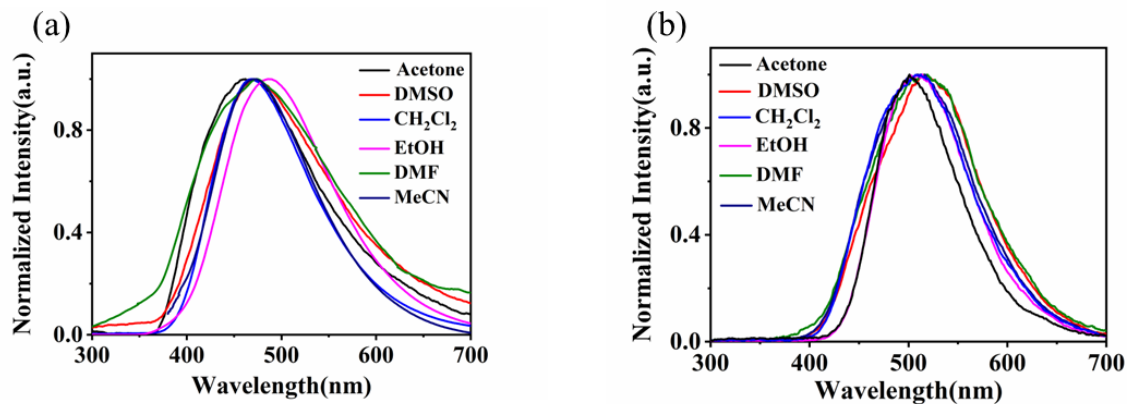


Figure S27. Normalized prompt (a) and delayed (b) emission spectra of **3** after soaked in different solvents.

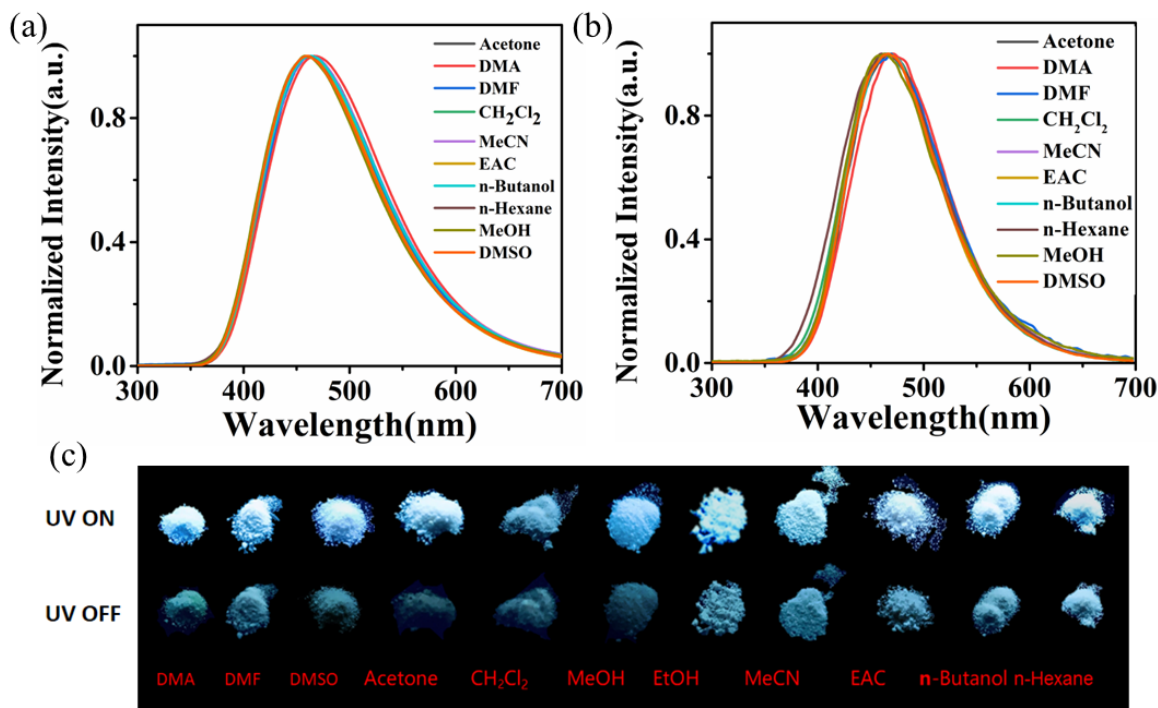


Figure 28. Normalized prompt (a) and delayed (b) emission spectra of **1** upon exposure to different solvents vapors. (c)

Luminescence photographs of **1** after exposed in different solvents vapors before and after turning off the UV excitation.

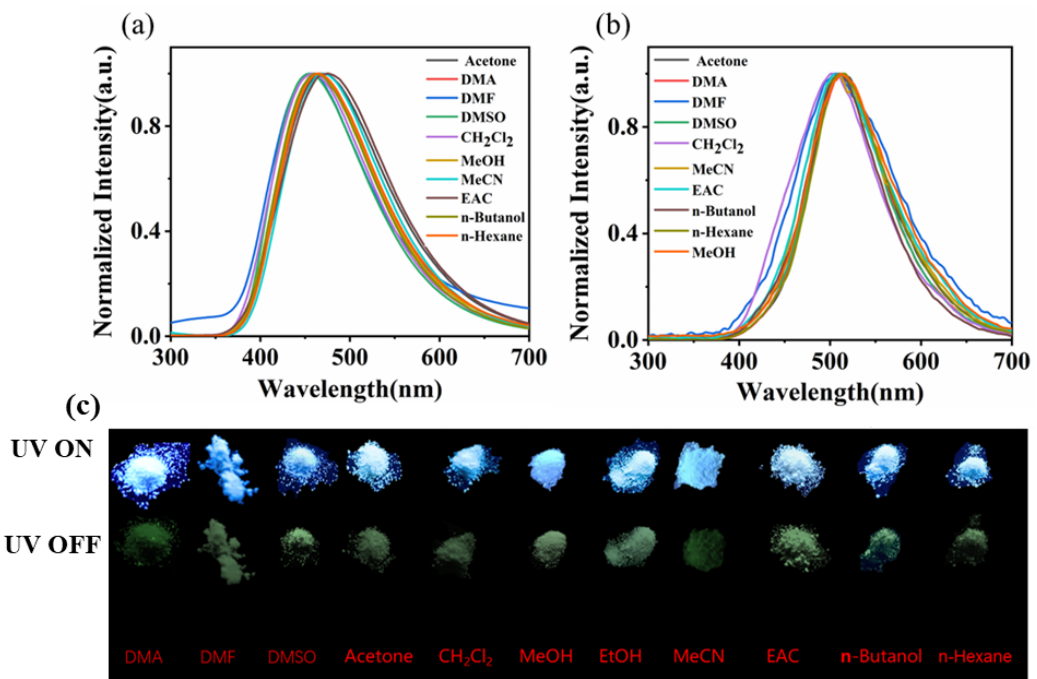


Figure 29. Normalized prompt (a) and delayed (b) emission spectra of **2** upon exposure to different solvents vapors. (c) Luminescence photographs of **2** after exposed in different solvents vapors before and after turning off the UV excitation.

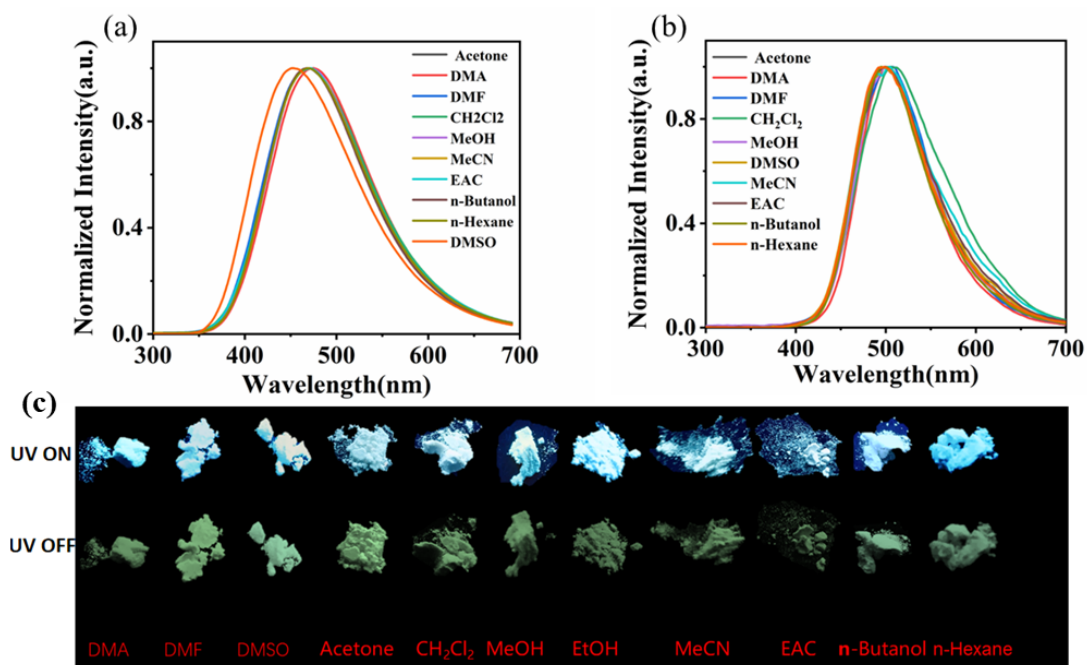


Figure 30. Normalized prompt (a) and delayed (b) emission spectra of **3** upon exposure to different solvents vapors. (c) Luminescence photographs of **3** after exposed in different solvents vapors before and after turning off the UV excitation.

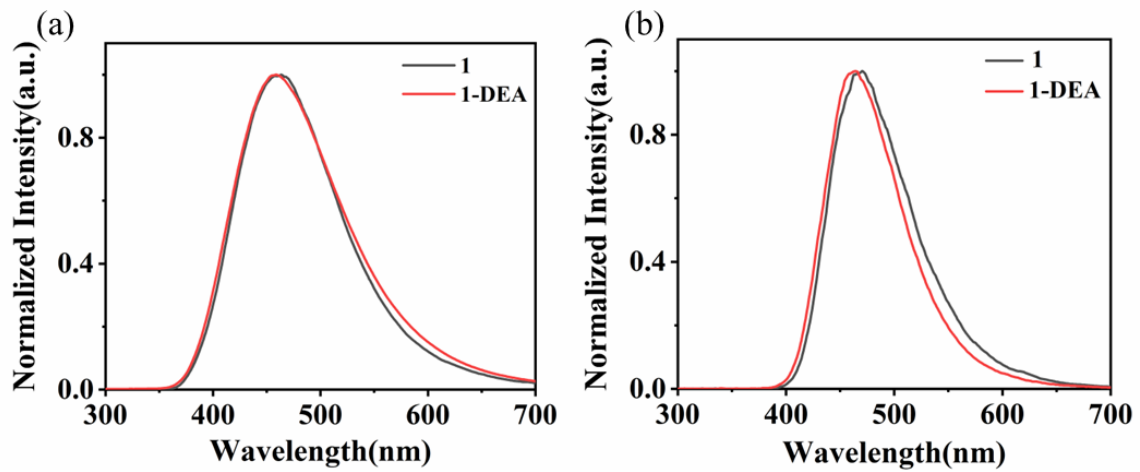


Figure S31. Normalized prompt (a) and delayed (b) emission spectra of **1** and **1** upon exposure to diethylamine vapor.

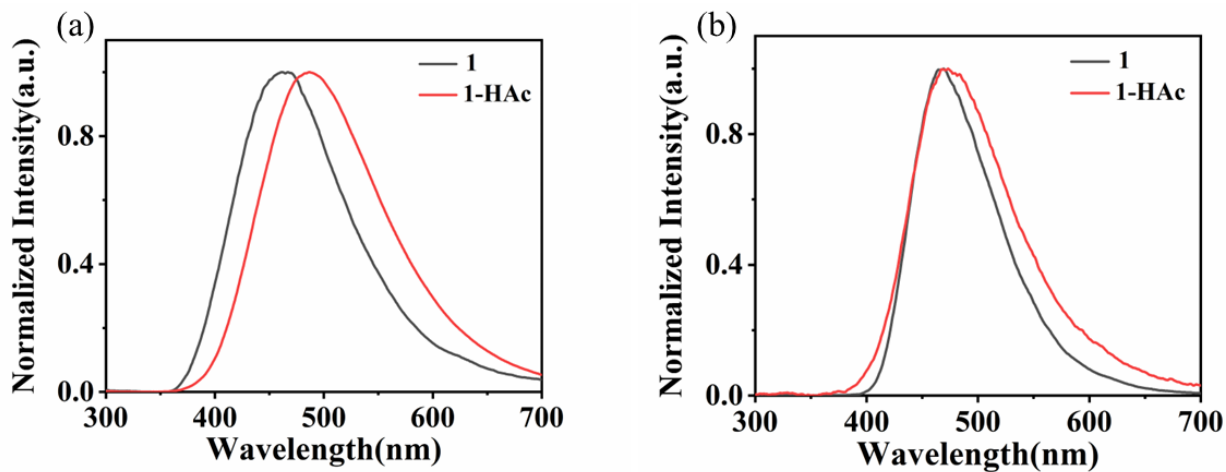


Figure S32. Normalized prompt (a) and delayed (b) emission spectra of **1** and **1** upon exposure to acetic acid vapor.

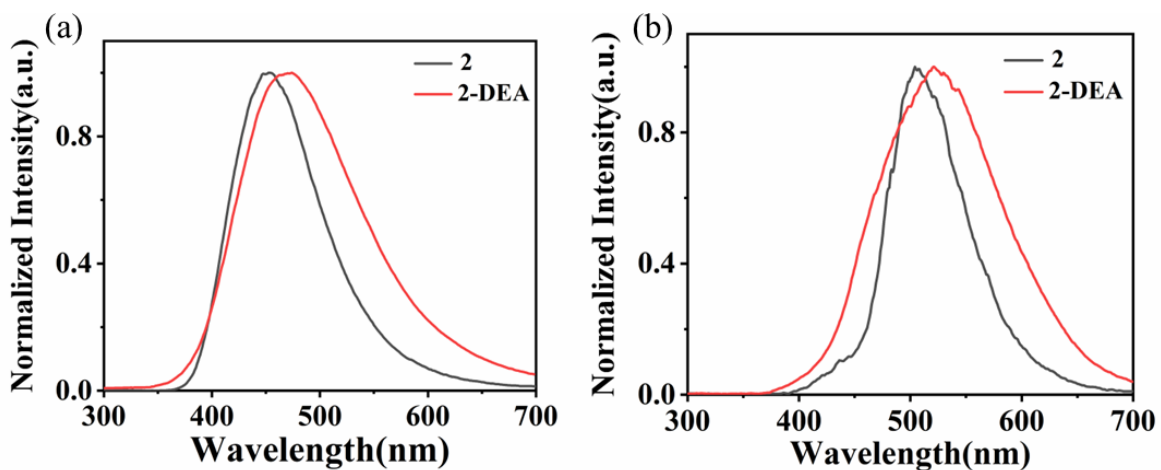


Figure S33. Normalized prompt (a) and delayed (b) emission spectra of **2** and **2** upon exposure to diethylamine vapor.

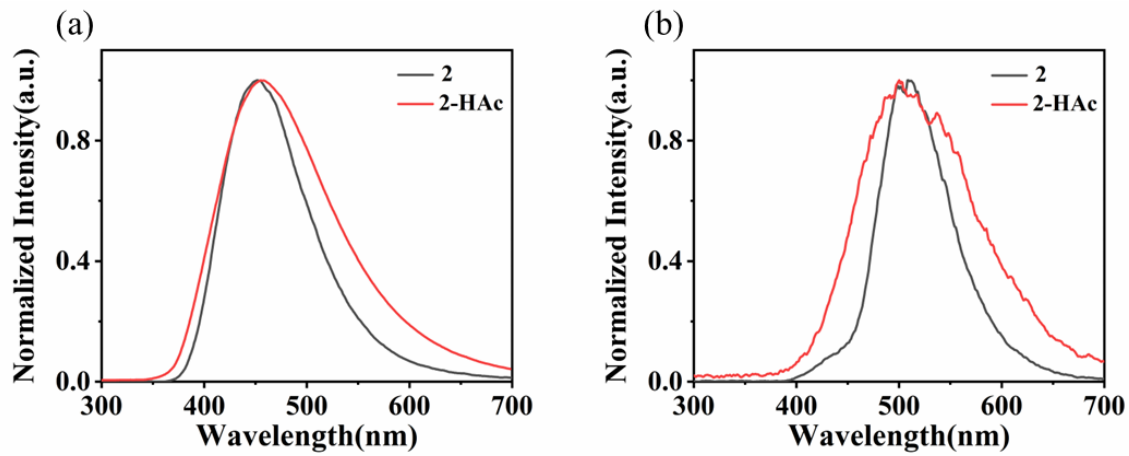


Figure S34. Normalized prompt (a) and delayed (b) emission spectra of **2** and **2** upon exposure to acetic acid vapor.

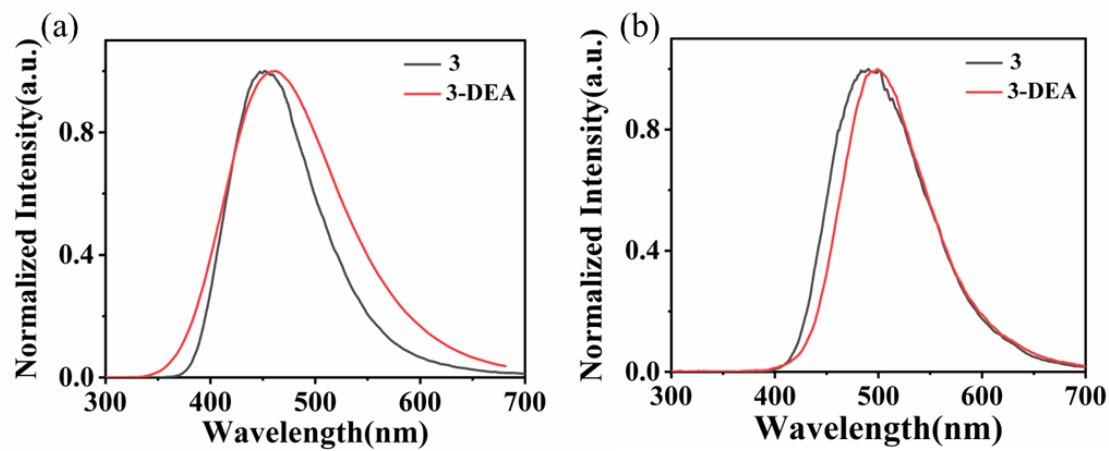


Figure S35. Normalized prompt (a) and delayed (b) emission spectra of **3** and **3** upon exposure to diethylamine vapor.

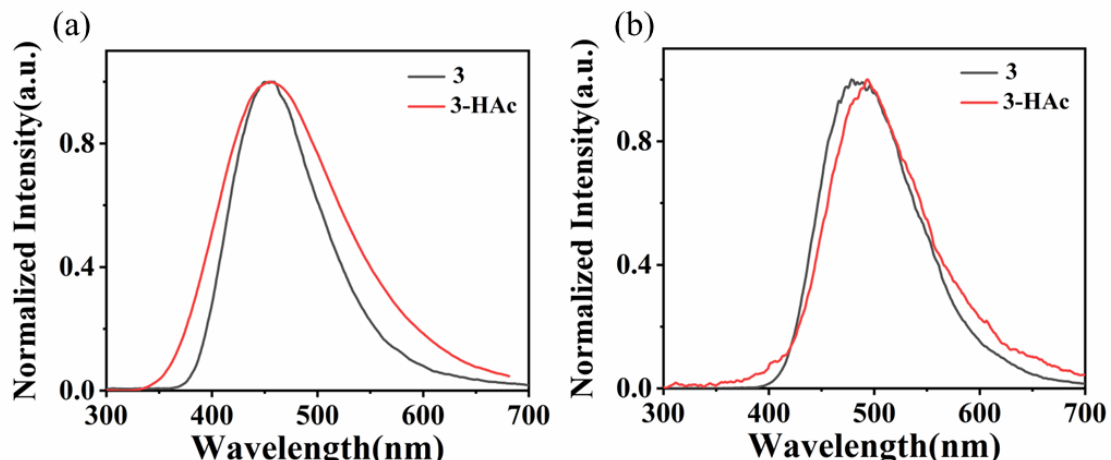


Figure S36. Normalized prompt (a) and delayed (b) emission spectra of **3** and **3** upon exposure to acetic acid vapor.

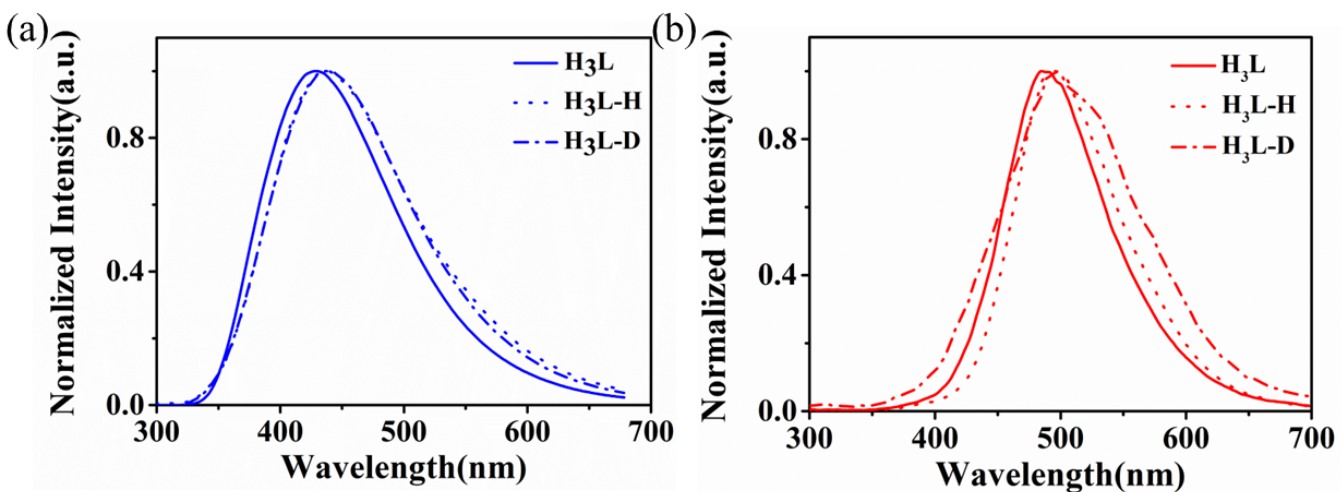


Figure S37. Normalized prompt (a) and delayed (b) emission spectra of H_3L , $\text{H}_3\text{L-H}$ (H_3L fumigated by water vapor) and $\text{H}_3\text{L-D}$ ($\text{H}_3\text{L-H}$ fumigated by DMSO vapor).

Reference:

1. G. M. Sheldrick, , Crystal Structure Refinement with SHELXL, *Acta. Cryst.*, 2015, **71**, 3-8.
2. Dmol³ Module, MS Modeling, Version 2.2, Accelrys Inc.: San, Diego, 2003.
3. B. Delley, An all-electron numerical method for solving the local density functional for polyatomic molecules, *J. Chem. Phys.*, 1990, **92**, 508-517.
4. J. P. Perdew, J. A. Chevary, S. H. Vosko, K. A. Jackson, M. R. Pederson, D. J. Singh and C. Fiolhais, Atoms, molecules, solids, and surfaces: Applications of the generalized gradient approximation for exchange and correlation, *Physical Review B*, 1992, **46**, 6671-6687.
5. B. Delley, From molecules to solids with the DMol³ approach, *J. Chem. Phys.*, 2000, **113**, 7756-7764.
6. Y. Zhao and D. G. Truhlar, The M06 suite of density functionals for main group thermochemistry, thermochemical kinetics, noncovalent interactions, excited states, and transition elements: two new functionals and systematic testing of four M06-class functionals and 12 other functionals, *Theor. Chem. Acc.*, 2007, **120**, 215-241.
7. K. Guzow, M. Milewska, C. Czaplewski and W. Wiczk, A DFT/TD DFT study of the structure and spectroscopic properties of 5-methyl-2-(8-quinolinyl)benzoxazole and its complexes with Zn(II) ion, *Spectrochim Acta A Mol Biomol Spectrosc*, 2010, **75**, 773-781.
8. M. J. Frisch, G. W. Trucks, H. B. Schlegel, G. E. Scuseria, M. A. Robb, J. R. Cheeseman, G. Scalmani, V. Barone, B. Mennucci, G. A. Petersson, H. Nakatsuji, M. Caricato, X. Li, H. P. Hratchian, A. F. Izmaylov, J. Bloino, G. Zheng, J. L. Sonnenberg, M. E. M. Hada, K. Toyota, R. Fukuda, J. Hasegawa, M. Ishida, T. Nakajima, Y. Honda, O. Kitao, H. Nakai, T. Vreven, J.A. Montgomery Jr., J.E. Peralta, F. Ogliaro, M. Bearpark, J. J. Heyd, E. Brothers, K. N. Kudin, V. N. Staroverov, R. Kobayashi, J. Normand, K. Raghavachari, A. Rendell, J. C. Burant, S. S. Iyengar, J. Tomasi, M. Cossi, N. Rega, J.M. Millam, M. Klene, J.E. Knox, J.B. Cross, V. Bakken, C. Adamo, J. Jaramillo, R. Gomperts, R.E. Stratmann, O. Yazyev, A.J. Austin, R. Cammi, C. Pomelli, J. W. Ochterski, R. L. Martin, K. Morokuma, V. G. Zakrzewski, G.A. Voth, P. Salvador, J. J. Dannenberg, S. Dapprich, A. D. Daniels, Ö. Farkas, J. B. Foresman, J. V. Ortiz, J. Cioslowski and D. J. Fox, *Gaussian 16, Revision A.03*, Gaussian Inc., Wallingford CT, 2016.
9. E. Papajak, J. Zheng, X. Xu, H. R. Leverenz and D. G. Truhlar, Perspectives on basis sets beautiful: seasonal plantings of diffuse basis functions, *J. Chem. Theory Comput.*, 2011, **7**, 3027-3034.
10. J. Zheng, X. Xu and D. G. Truhlar, Minimally augmented karlsruhe basis sets, *Theor. Chem. Acc.*, 2011, **128**, 295-305.

11. S. Grimme, J. Antony, S. Ehrlich and H. Krieg, A consistent and accurate ab initio parametrization of density functional dispersion correction (DFT-D) for the 94 elements H-Pu, *J. Chem. Phys.*, 2010, **132**, 154104.
12. T. Lu and F. Chen, Multiwfn: a multifunctional wavefunction analyzer, *J. Comput. Chem.*, 2012, **33**, 580-592.
13. W. Humphrey, A. Dalke and K. Schulten, VMD: Visual molecular dynamics, *J. Mol. Graphics*, 1996, **14**, 33-38.